A new consensus-based control strategy for intelligent cooperative buildings in microgrid*

Jaime López Pay and Raúl Mario del Toro Matamoros[1]

Abstract— **This work contains the development and validation through simulation of a new control strategy for intelligent cooperation between buildings in micro-grids. This strategy is responsible of managing the energy of each building, entailing the calculation of solar generation power, power exchange with the grid, available power for the loads and the charging/discharging of the batteries. The objective of the controller is to improve the efficiency of the whole micro-grid by fomenting the cooperation between buildings via power exchange. The strategy is developed using a System of Systems approach and is based on distributed algorithms that employ cooperative control techniques for consensus decision-making. The control architecture is based on a two-layer controller. The first layer is a model predictive controller (MPC) that calculates a reference for the system's behavior each hour using generation and demand predictions. The second layer is a controller that operates the system in *real time* by adjusting the reference given the actual values of demand and generation. The algorithm is validated using MatLAB as a simulation environment and GridLAB-D to obtain the generation and load profiles.**

I. INTRODUCTION

Intelligent cooperation between buildings involves the optimal management of the energy generation and storage capacity of solar self-consumption systems installed in these buildings. It would enhance collective self-consumption by utilizing surplus production in buildings with different load patterns [1]. For example, the high energy demand in office buildings during peak photovoltaic energy production hours can be met with surplus energy from neighboring residential buildings. Optimal management of generation capacity would also allow for optimizing the area used for photovoltaic panel installation and utilizing areas near consumers, such as building rooftops.

From a systems engineering perspective, a photovoltaic distributed renewable energy systems (DRES) and interconnected buildings can be considered as a System of Systems (SoS) [2]. This is because each building or home can be considered an independent system with its own internal energy consumption demands and dynamics. In contrast, solar self-consumption systems have a different dynamic, determined primarily by variations in weather conditions and solar radiation, but they are required to supply the energy demand of the building. Both systems, when integrated and interconnected to a distribution system or microgrid, can be considered a System of Systems. This consideration would allow the application of engineering methods that exploit the distributed and heterogeneous nature of the systems that comprise it, such as cooperative control in SoS to design distributed energy management solutions.

Cooperative control in SoS can be achieved using a consensus-based decision-making approach, thereby maximizing the benefits for each system [2]. This approach creates a set of interconnected systems, each pursuing its own objectives as well as common goals, through communication between them.

The use of consensus based techniques for control in microgrids has been studied in recent years by many researchers to solve short-time scale problems [3, 4, 5, 6, 7]. Several objectives can be achieved this way by the transmission of just one virtually defined state variable [8]. Energy management systems (EMS) are in charge of The optimal scheduling of distributed renewable-based energy systems and choosing which source is used. This can be done in real time [9], however, most EMS plan on a day ahead basis using predictions of generation and load [1, 10]. Many of this EMS include demand side management (DSM) techniques that allow more operational flexibility of the power systems [11, 12, 13, 14]. The day ahead nature of most EMS incentives the use of model predictive control (MPC) techniques [15, 16, 17]. EMS can use a centralized agent to coordinate different agents in charge of local control [18, 19]. Or even in a fully distributed manner [20, 21]. However, in the bibliography was not found a fully distributed multi-objective algorithm that managed the energy resources and needs of an isolated 100% renewable-based MG composed of several buildings with PV installations and BESS in the building scale for long term planning as well as short term adjustments due to predictions errors. A fully distributed solution, compared to less distributed or centralized solutions, offers advantages such as scalability, fault tolerance, improved performance by distributing the computing load and data processing, and greater local autonomy, among others [6].

In this work we propose a fully distributed consensus based control for the EMS of renewable based microgrids. It employs DSM techniques and is composed of two layers, a MPC layer for the day ahead scheduling and a second fast acting layer that adjusts the functioning to real time conditions. Both layers will pursue several objectives by the consensus of a single state variable.

The rest of this paper is organized as follows. Section II

*This work has been funded by the ECS4DRES project, which is supported by the Chips Joint Undertaking under grant agreement number 101139790 and its members, including the top-up funding by Germany, Italy, Slovakia, The Netherlands and Spain through MI-CIU/AEI/10.13039/501100011033/UE.

[1]Jaime López Pay and Raúl Mario del Toro Matamoros are with Center of Automation and Robotics, Spanish National Research Council, Arganda del Rey, Madrid, 28500, Spain {jaime.lopez,raul.deltoro}@car.upm-csic.es

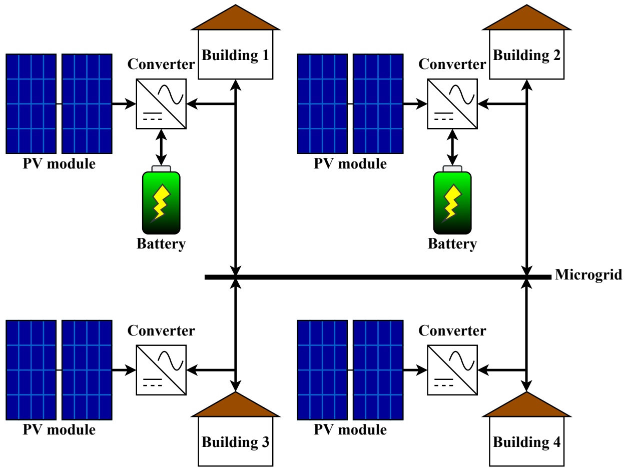

Fig. 1: Solar self-consumption microgrid overview

explains the control algorithms developed. Section III shows the results of said simulations and section IV finalizes with a conclusion.

II. CONTROL SYSTEM DESIGN

In any power system it is crucial to control the power injected in order to provide energy to the loads. In an isolated microgrid composed of building with PV self-consumption capabilities, such as that in figure 1, the only source of energy are the PV panels and their generation capabilities depend on the hour of the day. Therefore, energy storage systems (such as batteries) and their control are required. Furthermore, PV generation also depends on weather conditions and there can be long periods of time with very low generation, if we do not control the load batteries would deploy completely and total blackout would occur.

All in all, we need to control the PV generation, the charge/discharge and state of charge (SoC) of the battery, the power exchanged between buildings and the demand of each building with the objective of improving the system efficiency and avoid complete blackouts.

A. *Controller overview*

The control algorithm is composed of two different controllers that work in two different time frames. On one hand, we have a MPC that calculates the optimal behavior of the system given predicted values of average hourly generation and load. On the other hand, the optimal hourly behavior is then taken by a different controller that adjusts them to match the *real-time* measurements, denominated as real-time controller (RTC). The control unit has two tasks:

- Calculate the **converters' power references** of the batteries, PV panels and AC grid.
- Calculate the **available power for the loads**. In order to maintain energy balance, sometimes load must be shed.

In figure 2, we observe the whole control architecture. The different colors represent when information is exchanged, blue represents once each MPC cycle (once each hour), green

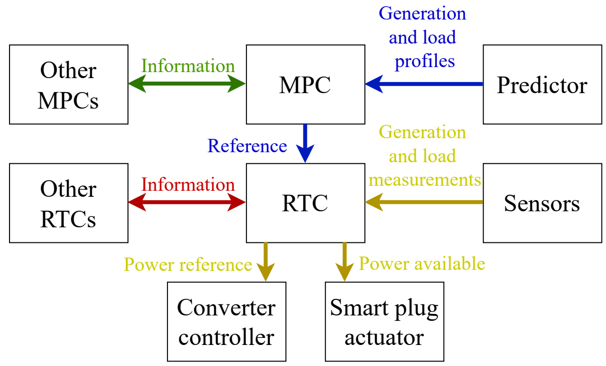

Fig. 2: Control architecture implementation

represents each MPC consensus iteration (several iterations per cycle), yellow represents once each RTC cycle (as fast as computation allows) and red represents each RTC iteration (several iterations per cycle).

B. *Model predictive control*

We will define an optimization problem for each building and a strategy that allows all buildings to cooperate and reach a consensus-based behavior.

1) Optimization problem: Each optimization problem is defined by its variables, constrains and objective function.

a) Variables and parameters: All variables are defined for each time k in the prediction horizon K and each building i and presented in table I with the parameters present in the constrains and objective function equations. We define a crucial load variable as high priority load (such as freezers or chargers), meaning that when shedding is needed the controller will shed non-crucial load first.

TABLE I: Optimization problem variables and parameters

Variable	**Symbol**	**Units**
Battery power (positive for charging)	$P_{bat}^{i,k}$	kW
Battery SoC (0 if there is no battery)	$SOC^{i,k}$	p.u.
Renewable generation	$P_{gen}^{i,k}$	kW
Non-crucial load provided	$P_{load}^{i,k}$	kW
Crucial load provided	$P_{crucial}^{i,k}$	kW
Parameter	**Symbol**	**Units**
Battery's maximum charge power	$P_{chargeMax}^{i}$	kW
Battery's maximum discharge power	$P_{dischargeMax}^{i}$	kW
Battery's maximum SoC	SOC_{max}^{i}	p.u.
Battery's minimum SoC	SOC_{min}^{i}	p.u.
Predicted solar available generation	$P_{available}^{i,k}$	kW
Predicted non-crucial demand	$P_{demand}^{i,k}$	kW
Predicted crucial demand	$P_{crucialDemand}^{i,k}$	kW
Maximum converter power	$P_{convMax}^{i}$	kW
Scheduled energy import	$P_{grid}^{i,k}$	kW
Initial SoC	$SOC^{i,0}$	p.u.
Battery capacity	C^{i}	kWh
Objective function weight vector	$(w_1^i, w_2^i, ..., w_5^i)$	p.u.
Installed solar capacity	$P_{solarMax}^{i}$	kW
Maximum demand	$P_{demandMax}^{i}$	kW

b) Constrains: The constrains define an energy model of each building. All constrains are defined for each time interval k in the prediction horizon.

$$-P^{i}_{dischargeMax} \leq P^{i,k}_{bat} \leq P^{i}_{chargeMax} \quad \forall k \qquad (1)$$
$$SOC^{i,k} \leq SOC^{i,k} \leq SOC^{i}_{max} \quad \forall k \qquad (2)$$
$$0 \leq P^{i,k}_{gen} \leq P^{i,k}_{available} \quad \forall k \qquad (3)$$
$$0 \leq P^{i,k}_{load} \leq P^{i,k}_{demand} \quad \forall k \qquad (4)$$
$$0 \leq P^{i,k}_{crucial} \leq P^{i,k}_{crucialDemand} \quad \forall k \qquad (5)$$
$$-P^{i}_{convMax} \leq P^{i,k}_{gen} - P^{i,k}_{bat} \leq P^{i}_{convMax} \quad \forall k \qquad (6)$$
$$-P^{i,k}_{gen} + P_{crucial} + P^{i,k}_{load} + P^{i,k}_{bat} = P^{i,k}_{grid} \quad \forall k \qquad (7)$$
$$SOC^{i,k} - SOC^{i,k-1} - \frac{P^{i,k}_{bat}}{C^{i}} = 0 \quad \forall k \qquad (8)$$

Where eq. (1) represents the battery power limits, eq. (2) the SoC limits, eq. (3) the solar generation limits, eqs. (4) and (5) the limits of the non-crucial and crucial load consumed, eq. (6) the converter power limits, eq. (7) the energy balance in the building and eq. (8) the change in the SoC. This last equation assumes a 1 h time interval and a 100% efficiency to allow the use of a simpler model and faster optimization.

c) Objective function: The objective function given by eq. (9) is the weighted sum of the objectives. The final SoC is maximized by the first component. The second component minimizes generation curtailment. The crucial and non-crucial load shedding is minimized by the third and fourth components. Finally, the last component minimizes the battery health degrading by minimizing its use.

$$\begin{aligned} F^{i} = \quad & w^{i}_{1} \cdot (-SOC^{i,K}) \quad + \\ & w^{i}_{2} \cdot \sum_{k=1}^{K} \frac{(P^{i,k}_{gen} - P^{i,k}_{available})^2}{(P^{i}_{solarMax})^2} \quad + \\ & w^{i}_{3} \cdot \sum_{k=1}^{K} \frac{(P^{i,k}_{crucial} - P^{i,k}_{crucialDemand})^2}{(P^{i}_{demandMax})^2} \quad + \\ & w^{i}_{4} \cdot \sum_{k=1}^{K} \frac{(P^{i,k}_{load} - P^{i,k}_{demand})^2}{(P^{i}_{demandMax})^2} \quad + \\ & w^{i}_{5} \cdot \sum_{k=1}^{K} \frac{(P^{i,k}_{bat})^2}{(P^{i}_{dischargeMax})^2} \end{aligned} \qquad (9)$$

2) Consensus value: We define a state variable that we want to reach consensus as the *available energy* value $y^{i,k}$ in eq. (10), taking into account several factors.

$$\begin{aligned} y^{i,k} = \quad & w^{i}_{1} \cdot \frac{SOC^{i,k} - SOC^{i}_{min}}{SOC^{i}_{max} - SOC^{i}_{min}} \quad + \\ & w^{i}_{2} \cdot \frac{P^{i,k}_{available} - P^{i,k}_{gen}}{P^{i}_{solarMax}} \quad + \\ & w^{i}_{3} \cdot \frac{P^{i,k}_{crucial} - P^{i,k}_{crucialDemand}}{P^{i}_{loadMax}} \quad + \\ & w^{i}_{4} \cdot \frac{P^{i,k}_{load} - P^{i,k}_{demanded}}{P^{i}_{loadMax}} \end{aligned} \qquad (10)$$

The first component represents the charge left on the battery and the second curtailed generation, both additional energy that can be provided to other buildings. The last two represent the shed load and thus energy deficit so they have negative values. All values are normalized and multiplied by their corresponding objective function weight.

3) Control signal: To reach consensus we need to relate the state variable $y^{i,k}$ to a control signal in a integrator-like dynamic. In our case the dynamical system is subsequent instances of the predictive model, solving the optimization problem of each building while adjusting it each time until consensus is reached. As we are running iterations, we will have a *discrete time system* where $[m]$ represents the iteration. We adjust the optimization by changing the scheduled energy exchange $P^{i,k}_{grid}[m]$ using equation 11, where g_{MPC} is the control signal gain.

$$\begin{aligned} P^{i,k}_{grid}[m] = & P^{i,k}_{grid}[m-1] + \\ & g_{MPC} \sum_{j \in N, i \neq j} a_{ij}(y^{j,k}[m-1] - y^{i,k}[m-1]) \end{aligned} \qquad (11)$$

4) Additional considerations:

a) Unfeasible iterations: Energy exchanged with the grid is currently not limited by eq. (11). However, we could obtain a value outside of its limits, making the optimization unfeasible. The upper bound is the load demand and maximum battery charge power at that time. The lower bound is the maximum generation and battery discharge power at that time. To avoid this, we define these upper and lower limits and redistribute the difference between saturated and unsaturated values among the other buildings.

b) Straying from optimal point: We could converge to a point where the sum of the objective function values is bigger than one obtained in a previous iteration. To avoid this we implement a different termination condition other than consensus, given by eq. (12). We calculate the sum of all objective functions for each iteration and compare it to the previous one. If we obtain a bigger value, we stop the loop and keep the previous optimization solution.

$$\sum_{i \in N} F^{i}[m] - \sum_{i \in N} F^{i}[m-1] \geq 0 \qquad (12)$$

5) Consensus optimization algorithm: The control algorithm for the MPC can be observed on Fig. 3. We first read the predictions for generation and demand. We then solve the individual optimization problems of each building and communicate the necessary data to neighboring buildings. We then calculate the next scheduled power exchange. We repeat until the condition given by eq. (12) is met. When the loop ends we return the previous result with the optimal schedule of each building for the next time-steps in the prediction horizon.

C. Real-time adjustment control

We implement a real-time controller (RTC) to adjust the reference obtained by the MPC to the *real* plant where the actual values of generation and demand may differ from the

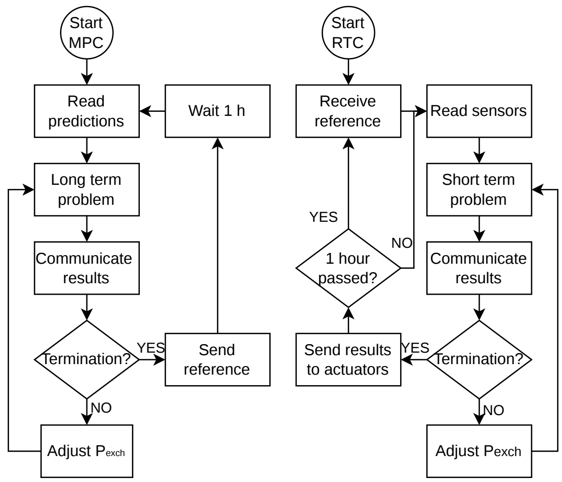

Fig. 3: Algorithm flowchart

predicted values. Its flowchart can be seen in fig. 3, having some differnces with respect to the MPC.

1) Optimization problem: The main difference with respect to the MPC optimization problem is that we have only one time-step. This means that all variables and parameters that had a k super-index do not have it.

a) Constrain relaxation.: Most constraints remain the same as in eqs. (1) to (8). However, P^i_{grid} is no longer a parameter but a variable and we add a reference as a parameter to ensures that there is always a feasible solution. We implement an additional term in the objective function as expressed in eq. (13) with a very high weight w_6 so that both values practically match and energy balance is maintained.

$$f^i_6 = w^i_6 \cdot (P^i_{grid} - P^i_{gridRef})^2 \tag{13}$$

b) Time constant: The time steps are not 1 hour anymore so we need to modify eq. (8) to add the time step.

$$SOC^i = SOC^{i,0} - \frac{P^i_{bat}\Delta t}{C^i} \tag{14}$$

c) Reference values.: In order to use the results obtained by the MPC we set a reference value for the SoC. This change is reflected in the SoC component of the objective function as can be seen in eq. (15) and on its lower bound.

$$f^i_1 = -SOC^i + (SOC^i_{ref} - SOC^i)^2 \tag{15}$$

2) Consensus value: We utilize a similar consensus value to that in eq. (10), but without any k super-index. We also modify the SoC term as to follow the reference:

$$y^i_1 = \frac{SOC^i - SOC^i_{ref}}{SOC^i_{max} - SOC^i_{min}} \tag{16}$$

3) Control signal: The control signal is calculated the same way as in eq. (11), but we now have a different gain g_{RT} and no k super-index.

III. RESULTS

The study case mimics the facilities in the Center of Automation and Robotics of the Spanish Research Council in Arganda del Rey, consisting on 4 buildings with PV pannels and inverters, 2 of them also counting with a BESS. Each building has its own controller that communicates with the other controllers, as shown in figure 1. To run the simulation we solve all optimization problems using the MatLAB Optimization Toolbox, more specifically we use the quadprog function that uses the interior-point convex algorithm [22], [23]. The load and generation data were obtained using GridLAB-D[24], a simulation software focused on the design of smart grids. We obtained profiles for two different cases, the first week of winter and the first week of summer. For the generation profiles we use typycal meteorological data for our location obtained from the online tool PVGIS [25]. We added noise to the prediction data used in the MPC in order to create the *real* data for the RTC. The optimization parameters that depend on hardware and the final control parameters chosen are presented in table II.

To adjust the control gains we change their value and observe the evolution of the available energy of each building with each iteration. Figure 4 shows the available energy of the RTC for a timestep in winter. We can observe how for low values of the gain (0.01 to 0.1) buildings approach consensus gradually. The higher the gain the closer buildings get to reaching consensus, reaching it for $g_{RTC} = 0.1$. When increasing the gain over this value the changes are too big and some oscillations appear. This oscillations make the algorithm reach the termination conditions too soon and stop working before reaching consensus. Therefore, we choose $g_{RTC} = 0.1$ for winter. Doing a similar analysis for the summer week leads us to choose $g_{RTC} = 10$ for summer.

We choose the different optimization weights one by one by running simulations with different values for a weight and calculating the total load shedding (crucial and non crucial), total generation curtailment and average battery.

TABLE II: Study case hardware parameters and final controller parameters

Building	1 and 2		3 and 4	
$P^i_{chargeMax}$	7.6 kW		0.0 kW	
$P^i_{dischargeMax}$	7.6 kW		0.0 kW	
SOC^i_{max}	1.00 p.u.		0.00 p.u.	
SOC^i_{min}	0.05 p.u.		0.00 p.u.	
$SOC^{i,0}$	0.75 p.u.		0.00 p.u.	
C^i	9.6 kWh		0.0 kWh	
$P^i_{converterMax}$	3.0 kW			
$P^i_{solarMax}$	2.02 kW			
$P^i_{demandMax}$	0.5 kW			
Case	**Summer**	**Winter**	**Summer**	**Winter**
g_{MPC}	5	0.3	5	0.3
g_{RTC}	10	0.1	10	0.1
w^i_1	0.0004	0.0004	0	0
w^i_2	0.1295	0.1244	0.1299	0.1299
w^i_3	0.8632	0.8295	0.8658	0.8658
w^i_4	0.0041	0.0041	0.0043	0.0043
w^i_5	0.0026	0.0415	0	0

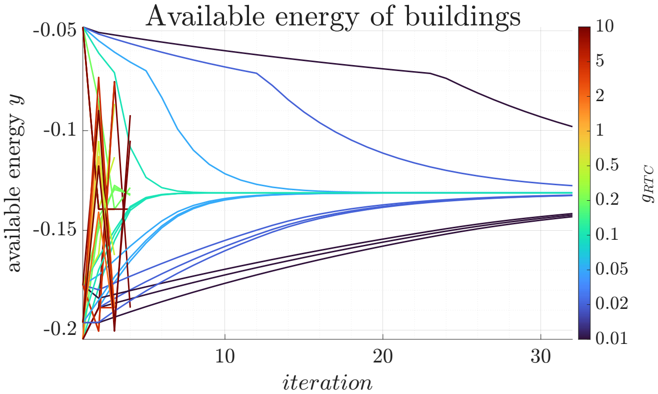

Fig. 4: Available energy evolution for the RTC in the first timestep of winter

Figure 5 shows the difference in the performance parameters between the initial (10) and other values for w_3 (before normalizing). We choose a value of 200 as we get the lowest crucial load shedding without a substantial increase in the other parameters. We perform a similar analysis for all other weights, but this is the one with the highest impact as it is also the biggest.

Then we perform a final simulation in summer and one in winter with those values. We represent the power balance on each building by plotting generation, battery discharge and microgrid power import in the positive axis and load, battery charge and microgrid power export in the negative axis. Figure 6 shows the power balance of buildings 1 and 3 during a week in winter and one in summer. The behavior of building 1 and 2 is really similar as they both have batteries, in the same way buildings 3 and 4 have almost equal behavior. In both weeks the buildings cooperate in the same way, at night power flow goes from buildings 1 and 2 to buildings 3 and 4, providing them with energy for their loads and during the day the power flow is reversed and buildings 3 and 4 are the ones providing energy for the loads of the whole microgrid while buildings 1 and 2 utilize their generation to recharge their batteries. However, a difference can be appreciated in the amount of load shed and energy

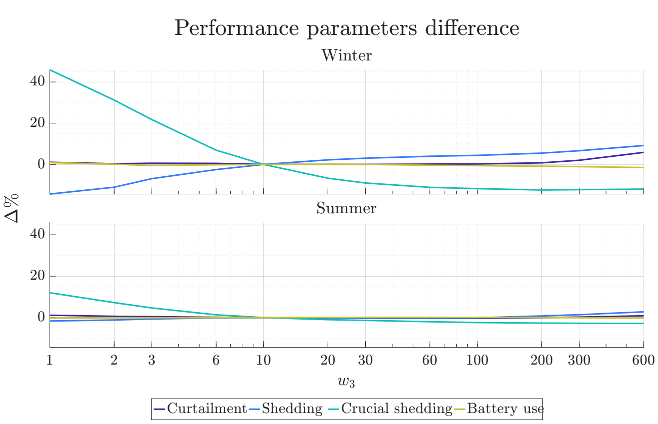

Fig. 5: Performance parameters for different values of w_3

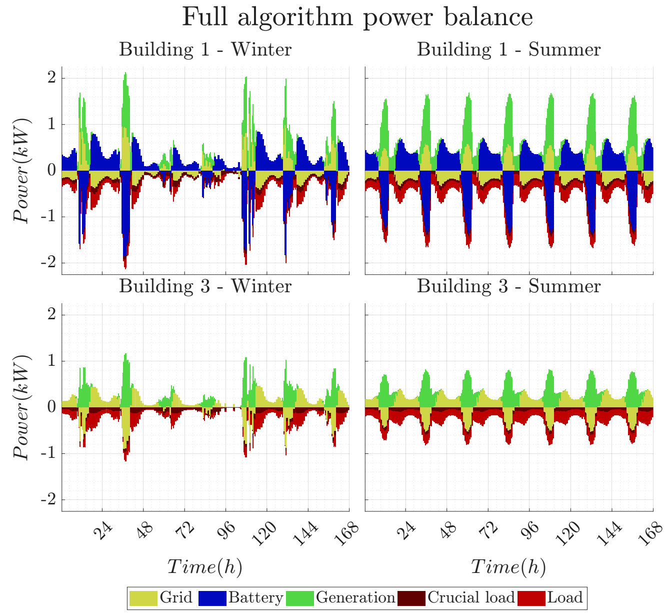

Fig. 6: Power balance in buildings 1 and 3 in winter and summer

generated. In summer, only 0.03 % of crucial load and 1.23 % of non-crucial load is shed during the whole week as we have more available generation than demand. While in winter the generation is not enough to cover all demand and is specially low on days 3 and 4. This means that at some points the non-crucial load has to be shed. In total, 9.23 % of crucial load and 55.86 % of non-crucial load is shed.

Finally, figure 7 shows the evolution of the SoC of the batteries in both winter and summer. We can observe how in summer we have a quite periodic behavior as SoC goes down at night until around 0.35 and then goes up, reaching

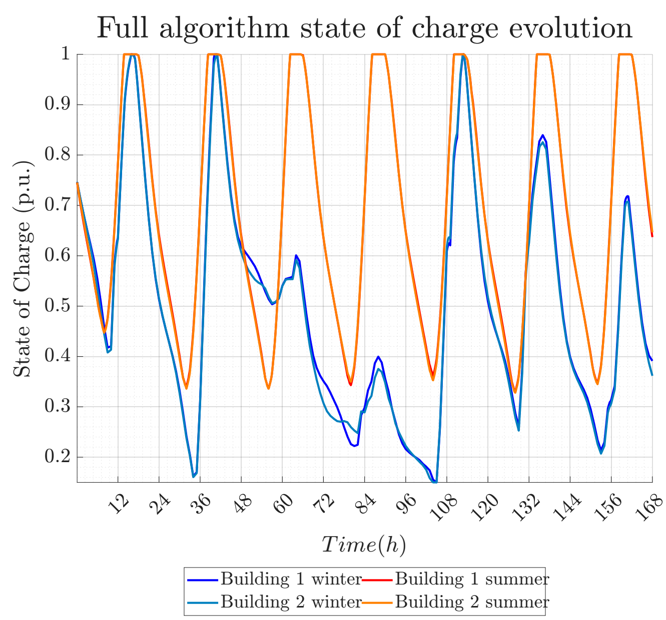

Fig. 7: SoC evolution

its maximum value for a couple of hours before there is need to discharge again. During this time PV generation needs to be reduced, leading to a total of 31.77 % of total available generation to be curtailed. However, in winter the discharge rate decreases on days 3 and 4. This is because the MPC predicts a lower generation day and thus needs to save energy and starts shedding non-crucial load in order to provide the crucial load. Even though the maximum SoC is not reached for long times we have a generation curtailment of 9.74 % of total available generation.

IV. CONCLUSIONS

This work proposes a new distributed control algorithm for energy management of buildings that foments cooperation. The approach used allows to define an unified consensus variable based on each system components and objectives, which gives potential to future expansions with more heterogeneous participants in the microgrid. The results provide a *prove of concept* for the algorithm, as it is able to manage solar generation, battery charge/discharge, energy exchange between buildings and load shedding in a distributed manner. The effect of the control signal gains and optimization weights, were analyzed by changing their values and observing the consensus capabilities of the algorithm and evaluating some performance parameters.

In summer we are able to reach almost perfect performance as the amount of load shed is negligible and the amount of generation curtailment cannot be avoided as batteries reach complete SoC. In winter results are good as the crucial load shed is much smaller than the non-crucial load shed and the controller is able to save energy during low generation periods. However, the performance could still be improved by trying to eliminate generation curtailment and crucial load shedding completely.

Some future steps are improving the decision making process to reduce unnecessary load shedding and generation curtailment. Additionally, making the model used more realistic by adding factors such as efficiency and dynamic limits of the batteries. These models will allow for a more thorough evaluation of the algorithm before its implementation and validation in physical laboratory infrastructures.

REFERENCES

[1] Ioannis Zenginis et al. "Optimal Power Equipment Sizing and Management for Cooperative Buildings in Microgrids". In: *IEEE Transactions on Industrial Informatics* 15.1 (2019), pp. 158–172.

[2] Thrishantha Nanayakkara, Ferat Sahin, and Mo Jamshidi. *Intelligent control systems with an introduction to system of systems engineering*. Taylor & Francis Group, 2010.

[3] Javad Khazaei and Dinh Hoa Nguyen. "Consensus Control of Distributed Battery Energy Storage Devices in Smart Grids". In: Feb. 2021. ISBN: 978-1-78985-877-8.

[4] Li Su et al. "Distributed energy grid control method based on collaborative consensus algorithm". In: *Energy Reports* 7 (2021). 2021 International Conference on Energy Engineering and Power Systems, pp. 1075–1083. ISSN: 2352-4847.

[5] Andrew Xavier Raj Irudayaraj et al. "Distributed intelligence for consensus-based frequency control of multi-microgrid network with energy storage system". In: *Journal of Energy Storage* 73 (2023), p. 109183. ISSN: 2352-152X.

[6] Majid Moradi, Mojtaba Heydari, and Seyed Fariborz Zarei. "An overview on consensus-based distributed secondary control schemes in DC microgrids". In: *Electric Power Systems Research* 225 (2023), p. 109870. ISSN: 0378-7796.

[7] Weihang Yan et al. "Consensus-Based Approach for Active Power Control and Reserve Estimation in Distributed PV Systems". In: *2022 IEEE Power & Energy Society General Meeting (PESGM)*. 2022, pp. 1–5.

[8] Jialei Su et al. "A simplified consensus-based distributed secondary control for battery energy storage systems in DC microgrids". In: *International Journal of Electrical Power & Energy Systems* 155 (2024), p. 109627. ISSN: 0142-0615.

[9] M.H. Elkholy et al. "Design and implementation of a Real-time energy management system for an isolated Microgrid: Experimental validation". In: *Applied Energy* 327 (2022), p. 120105. ISSN: 0306-2619.

[10] Mauricio Rodriguez, Diego Arcos–Aviles, and Wilmar Martinez. "Fuzzy logic-based energy management for isolated microgrid using meta-heuristic optimization algorithms". In: *Applied Energy* 335 (2023), p. 120771. ISSN: 0306-2619.

[11] Ramia Ouederni, Bechir Bouaziz, and Faouzi Bacha. "Advanced Techniques for Optimizing Demand-Side Management in Microgrids Through Load-Based Strategies". In: *International Journal of Advanced Computer Science and Applications* 15.10 (2024).

[12] Yaju Rajbhandari et al. "Enhanced demand side management for solar-based isolated microgrid system: Load prioritisation and energy optimisation". In: *IET Smart Grid* 7.3 (2024), pp. 294–313.

[13] Adel Merabet et al. "Optimization and energy management for cluster of interconnected microgrids with intermittent non-polluting and diesel generators in off-grid communities". In: *Electric Power Systems Research* 241 (2025), p. 111319. ISSN: 0378-7796.

[14] Jinyi Xu et al. "Optimization of demand side management strategies for building clusters based on cooperative game theory". In: *Journal of Physics: Conference Series* 2781.1 (June 2024), p. 012022.

[15] Roberto Bustos et al. "Hierarchical energy management system for multi-microgrid coordination with demand-side management". In: *Applied Energy* 342 (2023), p. 121145. ISSN: 0306-2619.

[16] Yan Zhang et al. "Robust model predictive control for optimal energy management of island microgrids with uncertainties". In: *Energy* 164 (2018), pp. 1229–1241. ISSN: 0360-5442.

[17] Javier Tobajas et al. "Resilience-oriented schedule of microgrids with hybrid energy storage system using model predictive control". In: *Applied Energy* 306 (2022), p. 118092. ISSN: 0306-2619.

[18] Yiming Wang et al. "Integration of smart buildings with high penetration of storage systems in isolated 100 % renewable microgrids". In: *Journal of Energy Storage* 105 (2025), p. 114633. ISSN: 2352-152X.

[19] Liwei Ju et al. "Multi-agent-system-based coupling control optimization model for micro-grid group intelligent scheduling considering autonomy-cooperative operation strategy". In: *Energy* 157 (2018), pp. 1035–1052. ISSN: 0360-5442.

[20] Ajay Kumar Sampathirao et al. "Distributed conditional cooperation model predictive control of interconnected microgrids". In: *Automatica* 157 (2023), p. 111258. ISSN: 0005-1098.

[21] Miguel A. Velasquez et al. "Hierarchical dispatch of multiple microgrids using nodal price: an approach from consensus and replicator dynamics". In: *Journal of Modern Power Systems and Clean Energy* 7 (6 2019), pp. 1573–1584.

[22] Sanjay Mehrotra. "On the Implementation of a Primal-Dual Interior Point Method". In: *SIAM Journal on Optimization* 2.4 (1992), pp. 575–601.

[23] Anna Altman and Jacek Gondzio. "Regularized Symmetric Indefinite Systems in Interior Point Methods for Linear and Quadratic Optimization". In: *Optimization Methods and Software* 11-12 (Jan. 1998), pp. 275–302.

[24] GridLAB-D. *GridLAB-D webpage*. URL: `https://www.gridlabd.org/`.

[25] European Commission. *PVGIS v5.3*. URL: `https://re.jrc.ec.europa.eu/pvg_tools/es/`.